ChemPubSoc Europe

DOI: 10.1002/cmdc.201500007

CHEMMEDCHEM Full Papers

Development of Urea and Thiourea Kynurenamine Derivatives: Synthesis, Molecular Modeling, and Biological Evaluation as Nitric Oxide Synthase Inhibitors

Mariem Chayah,[a] M. Dora Carrión,[a] Miguel A. Gallo,[a] Rosario Jiménez,[b] Juan Duarte,[b] and M. Encarnación Camacho*[a]

Herein we describe the synthesis of a new family of kynurenamine derivatives with a urea or thiourea moiety, together with their in vitro biological evaluation as inhibitors of both neuronal and inducible nitric oxide synthases (nNOS and iNOS, respectively), enzymes responsible for the biogenesis of NO. These compounds were synthesized from a 5-substituted-2-nitrophenyl vinyl ketone scaffold in a five-step procedure with moderate to high chemical yields. In general, the assayed compounds show greater inhibition of iNOS than of nNOS, with 1-[3-(2-amino-5-chlorophenyl)-3-oxopropyl]-3-ethylurea (compound **5n**) being the most potent iNOS inhibitor in the series and the most iNOS/nNOS-selective compound. In this regard, we performed molecular modeling studies to propose a binding mode for this family of compounds to both enzymes and, thereby, to elucidate the differential molecular features that could explain the observed selectivity between iNOS and nNOS.

Introduction

Nitric oxide (NO) is an important second-messenger molecule that regulates several physiological functions in the nervous, immune, and cardiovascular systems.[1] A family of nitric oxide synthase (NOS) enzymes catalyze the biosynthesis of NO using L-arginine (L-Arg) as a substrate. Native NOS is a homodimeric enzyme. Each monomer consists of an N-terminal oxygenase domain with a catalytic heme active site and a cofactor tetrahydrobiopterin binding site, and a C-terminal electron-donating reductase domain binding flavin adenine dinucleotide (FAD), flavin mononucleotide (FMN), and nicotinamide adenine dinucleotide (NADPH).[2,3] The linker between the two functional domains is a calmodulin binding motif that enables electron flow from the oxygenase domain to the reductase domain, catalyzing the oxidation of L-Arg to L-citrulline with concomitant production of NO.[4]

Three similar isoforms of NOS have been identified in mammals.[5] Neuronal NOS (nNOS) and endothelial NOS (eNOS) are constitutive and regulated by intracellular Ca^{2+}/calmodulin. They continually produce low levels of NO used for nerve function and blood regulation, respectively. Conversely, inducible NOS (iNOS) is expressed by macrophages and microglia, produces large toxic bursts of NO to fight pathogens, and is not Ca^{2+}-dependent.[6,7]

To exert appropriate functions, NO synthesis by the three isozymes is under tight regulation. The overproduction of NO by nNOS or iNOS and the underproduction by eNOS have been associated with several pathological processes, including neurodegenerative diseases such as Alzheimer's,[8] Parkinson's[9] or Huntington's,[10] as well as amyotrophic lateral sclerosis[11] and chronic inflammatory[12] and autoimmune diseases such as rheumatoid arthritis, multiple sclerosis, colitis,[13] hypertension,[14] and atherosclerosis.[15]

Accordingly, inhibition of nNOS or iNOS, but not of eNOS, could provide an effective therapeutic approach. Moreover, selective inhibitors could be useful pharmacological tools to investigate other biological functions of NO. The research objective of our group is to develop potent and selective nNOS or iNOS inhibitors. To this end, we have carried out the publication of several families of inhibitors, some with good inhibition and selectivity.

In previous experiments, we demonstrated that melatonin **1**, the hormone secreted by the pineal gland, produces inhibitory effects on the CNS in rats and humans.[16] These effects could be interpreted as resulting from the inhibition of NOS. In particular, it has been shown that melatonin inhibits the nNOS isoform in a dose-dependent and calmodulin-dependent manner.[17]

In addition, we have described several compounds with kynurenine **2**,[18] kynurenamine **3**,[19] and 4,5-dihydro-1*H*-pyrazole **4**[20] structures as nNOS inhibitors. The last compounds are rigid analogues of the main brain metabolite of melatonin, *N*-acetyl-5-methoxykynurenamine (**3**, $R^1 = OCH_3$, $R^2 = CH_3$), which also inhibits the iNOS in sepsis associated with Parkinson's dis-

[a] *M. Chayah, Dr. M. D. Carrión, Prof. M. A. Gallo, Dr. M. E. Camacho*
Departamento de Química Farmacéutica y Orgánica
Facultad de Farmacia, Universidad de Granada (Spain)
E-mail: ecamacho@ugr.es

[b] *Dr. R. Jiménez, Prof. J. Duarte*
Departamento de Farmacología
Facultad de Farmacia, Universidad de Granada (Spain)

Supporting information for this article is available on the WWW under http://dx.doi.org/10.1002/cmdc.201500007: characterization data for compounds **9b–c**, **9e**, **9g–h**, **9j**, **9l–m**, **9o**, **10b–c**, **10e**, **10g--h**, **10j**, **10l–m**, **10o**, **5b–c**, **5e**, **5g–h**, **5j**, **5l--m**, and **5o**.

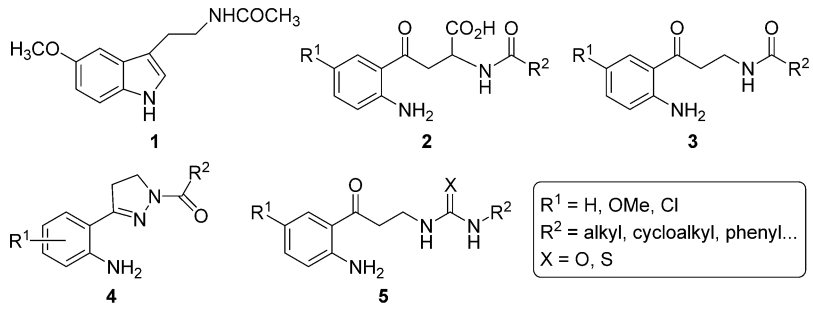

Figure 1. Melatonin and NOS inhibitors synthesized by our research group.

ease.[21] We have demonstrated that these pyrazole derivatives behave as nNOS/iNOS-selective inhibitors[22] (Figure 1).

In this paper, we report the synthesis and biological evaluation of a series of more flexible compounds (**5**). These products were designed from kynurenamine derivatives **3**, carrying a urea or thiourea substituted group, isosteric to the final guanidine moiety of the L-Arg, in order to find potent and selective inhibitors of NOS.

Results and Discussion

Chemistry

The synthesis of derivatives **5a–o** was carried out using the general methodology shown in Scheme 1. Compounds **7a–c** were synthesized as previously reported[19] from 2-nitrophenyl, 5-methoxy-2-nitrophenyl, and 5-chloro-2-nitrophenyl vinyl ketones **6a–c** by treatment with phthalimide in the presence of sodium methoxide to afford the *N*-(3-(2-nitro-5-substituted-phenyl)-3-oxopropyl)phthalimides. Protection of the resultant ketones by reaction with ethylene glycol in the presence of *p*-toluenesulfonic acid yielded dioxolane derivatives **7a–c**, respectively. Reaction of these derivatives with hydrazine opened the phthalimide moiety to give intermediates 2-(2-(5-substituted-2-nitrophenyl)-1,3-dioxolan-2-yl)-ethanamines (**8a–c**). Nucleophilic addition of either alkyl isocyanate or alkyl isothiocyanate[23] to these derivatives gave intermediates **9a–o** (60–96% yield) with an alkyl urea or thiourea residue, which led to ketones **10a–o** after acidification (61–94% yield). Finally, reduction of the nitro group belonging to the aromatic ring with $Fe/FeSO_4$ results in final kynurenamine derivatives **5a–o** (64–95% yield).

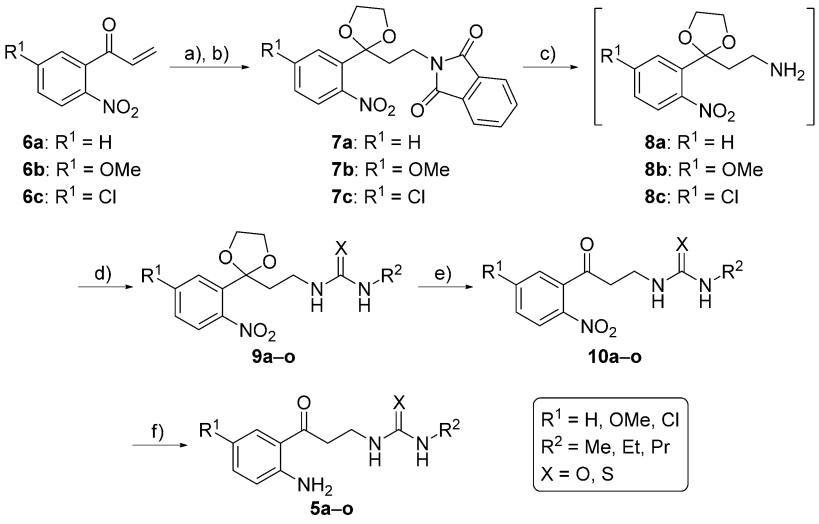

Scheme 1. Synthesis of kynurenamine derivatives **5a–o**. *Reagents and conditions*: a) Phthalimide, NaOMe, DMSO, RT, 2 h; b) $(CH_2OH)_2$, *p*-TsOH, toluene, reflux, 10 h; c) NH_2NH_2, dry EtOH, reflux, 4.5 h; d) $XCNR^2$, anhyd CH_2Cl_2, RT, overnight; e) HCl, CH_2Cl_2, RT, 4 h; f) $Fe/FeSO_4$, H_2O, 95 °C, 3 h.

Inhibition of iNOS and nNOS

The biological activity of new compounds **5a–o** as inhibitors of both iNOS and nNOS has been evaluated by means of in vitro assays using recombinant isoenzymes. The assays were performed with each compound at 1 mM to identify the most potent and selective derivatives. Furthermore, the IC_{50} values were measured for the most interesting compounds. Table 1 illustrates the inhibition percentages versus iNOS and nNOS (kynurenamine **3a**, previously described,[19] was introduced as a reference), and Figure 2 shows the percentages of residual activity of both isoforms in the presence of each compound. To interpret these biological results properly, we separately studied the effect of each substituent (R^1, R^2, and X) on the potency and/or selectivity of all resulting compounds.

In general, all compounds show better inhibition values for iNOS than for nNOS, with the chlorinated series having the most active compounds. Molecules with neutral ($R^1 = H$) or electron-donating ($R^1 = OCH_3$) phenyl substituents have lower inhibitory activity, indicating that an electron withdrawing group such as chloride is more suitable for the inhibition of both isoforms. Derivatives with a methylthiourea moiety (**5a**, **5f**, and **5k**) have, in general, good inhibition versus both isoforms, independently of the R^1 substituent.

When we compare urea and thiourea derivatives with the same R^2 substituent, the iNOS inhibitory effect decreases when the R^2 volume increases in series with $R^1 = H$ (**5b–c** and **5d–e**) and $R^1 = Cl$ (**5l–m** and **5n–o**), while in the series with $R^1 =$ OMe, iNOS inhibition increases

Table 1. In vitro iNOS and nNOS inhibition observed in the presence of compounds **5a–o**.

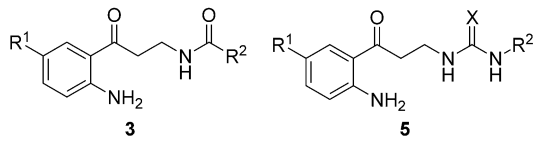

3 **5**

Compd	R^1	R^2	X	Inhibition [%][a] iNOS	nNOS
3a	OMe	Me	–	30.90 ± 2.92	65.36 ± 5.60[b]
5a	H	Me	S	71.71 ± 2.43	77.67 ± 1.02
5b	H	Et	S	45.83 ± 1.73	12.93 ± 3.45
5c	H	Pr	S	38.88 ± 3.59	47.48 ± 2.97
5d	H	Et	O	50.93 ± 3.85	11.80 ± 0.39
5e	H	Pr	O	38.03 ± 3.72	18.25 ± 0.87
5f	OMe	Me	S	78.20 ± 2.43	46.04 ± 2.85
5g	OMe	Et	S	17.71 ± 2.74	40.30 ± 0.32
5h	OMe	Pr	S	39.30 ± 0.99	47.21 ± 1.23
5i	OMe	Et	O	22.08 ± 1.57	0.47 ± 3,34
5j	OMe	Pr	O	55.28 ± 1.24	14.64 ± 0.65
5k	Cl	Me	S	51.29 ± 1.32	60.84 ± 0.82
5l	Cl	Et	S	77.86 ± 1.08	69.78 ± 1.05
5m	Cl	Pr	S	51.91 ± 1.28	53.42 ± 1.46
5n	Cl	Et	O	78.63 ± 1.34	9.86 ± 3.17
5o	Cl	Pr	O	59.58 ± 2.34	74.08 ± 1.04

[a] Values are the mean ± SEM of the percentage of iNOS and nNOS inhibition produced by each compound at 1 mM, determined from three experiments performed in triplicate using recombinant iNOS and nNOS enzymes. [b] Kynurenamine **3a** was used as a reference; see ref. [19].

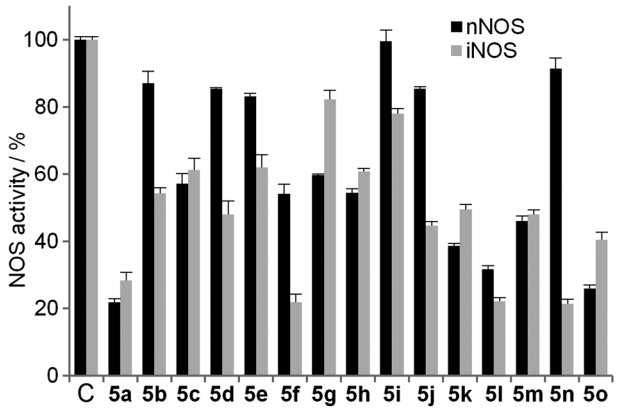

Figure 2. Residual activities of nNOS and iNOS in the presence of tested kynurenamine derivatives (compounds **5a–o**) at 1 mM, as compared with those of untreated samples (C). Each value is the mean ± SEM of three experiments performed in triplicate using recombinant iNOS and nNOS enzymes.

with the volume of R^2 (**5g–h** and **5i–j**). On the other hand, nNOS inhibition values increase with the volume of the R^2 substituent from an ethyl to a propyl group, with the exception of **5l–m**, for which the opposite is true.

In this new family of kynurenamines, the urea residue plays an important role in compound selectivity. All compounds with a urea group inhibit iNOS to a greater extent than nNOS, except **5o**. This effect can be observed clearly in compound **5n** which, besides having very good inhibitory activity, had eightfold selectivity for iNOS over nNOS. Table 2 shows the IC_{50} values of the most interesting synthesized kynurenamine derivatives for both isoenzymes. Compounds **5f** and **5n** had the best results versus iNOS, confirming the potency and selectivity of **5n**. With respect to nNOS, **5a** showed the best IC_{50} value.

Table 2. Inhibition of nNOS and iNOS activity by compounds **5a**, **5f**, **5l**, **5n**, and **5o**.

Compd	IC_{50} [mM][a] nNOS	iNOS
5a	0.18	0.58
5f	–[b]	0.11
5l	0.59	0.59
5n	–[b]	0.10
5o	0.43	0.86

[a] Data obtained by measuring percent inhibition with at least five inhibitor concentrations. [b] Not tested.

Effects of 5n on LPS-induced vascular hyporeactivity to noradrenaline (NA) and eNOS inhibition

The most interesting compound in this family was **5n.** To test functional evidence and to ensure the iNOS selectivity of this compound, we performed a pharmacological essay, using descending thoracic aortic rings. LPS inhibited agonist-induced contractions of isolated vascular preparations.[24] This effect is related to NO overproduction from the induction of iNOS in vascular smooth muscle. In fact, aminoguanidine, a preferential inhibitor of iNOS, reverses the blunted phenylephrine-evoked contraction of endothelium-denuded aortic rings from LPS-treated rats or rings exposed to LPS in vitro. Aminoguanidine did not impair the relaxation of aortic rings with endothelium to acetylcholine, a known stimulator of eNOS.[25] As shown in Figure 3a, incubation of endotoxin decreased the contractile responses elicited by NA in aortic rings without endothelium. Incubation of aortic rings with the NOS inhibitor L-NAME significantly restored NA responses from the LPS group, showing that NO is involved in the attenuated vascular reactivity to NA induced by endotoxin (Figure 3b). Furthermore, the presence of **5n** partially prevented endotoxin-induced NA contractile hyporesponsiveness.

We also carried out an eNOS inhibitory activity assay for **5n**, using human umbilical vein endothelial cells (HUVECs) incubated with 1 mM of **5n** or vehicle and measuring the NO production stimulated by the known eNOS activator A23187. This agent increased NO production in a time-dependent manner. No significant differences ($p > 0.05$) were observed in A23187 stimulated NO production in the presence of **5n**, showing that this compound did not inhibit eNOS (Figure 3c). Moreover, the endothelium-dependent relaxation by acetylcholine was not affected by **5n** (Figure 3d), confirming the absence of eNOS inhibition by this compound.

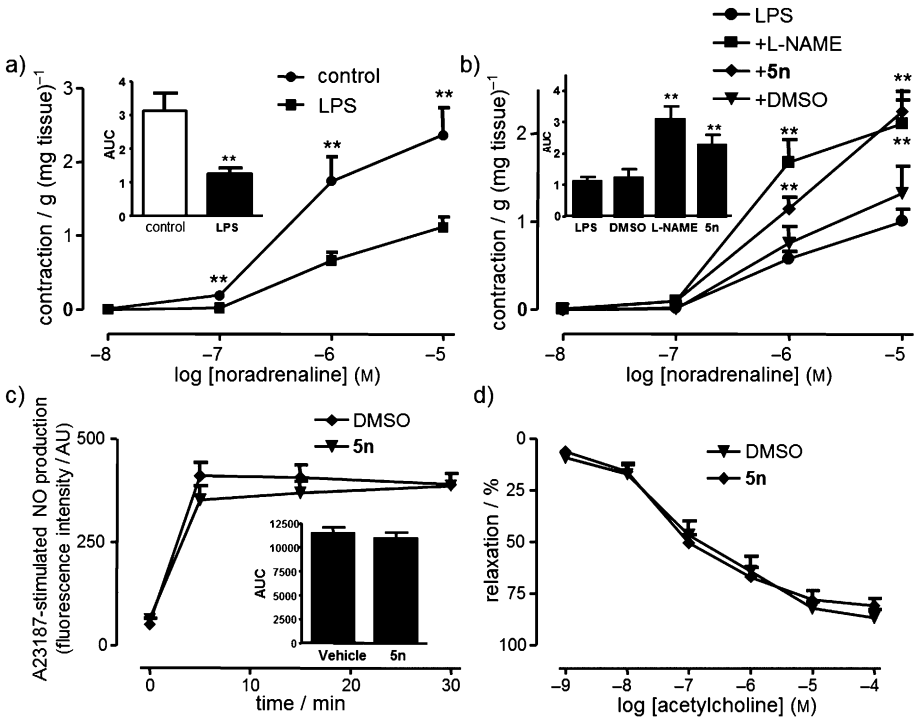

Figure 3. Effects of **5n** on NA-induced contraction in LPS-treated rings and eNOS activation. NA-evoked contraction of rat aortic rings ($n=6$–8) without endothelium treated in vitro: a) with or without LPS (1 μg mL^{-1}, 20 h), or b) in the presence or absence of L-NAME (3×10^{-4} M), **5n** (10^{-4} M), or DMSO, 30 min before NA. c) A23187-dependent NO production in HUVECs incubated with DMSO or **5n** (1 mM) for 30 min ($n=12$). d) Acetylcholine-evoked relaxation in aortic rings with endothelium contracted with 1 μM NA in the presence of DMSO or **5n** (1 mM) for 30 min ($n=5$). Data are expressed as the mean ± SEM of n experiments; $^{**}p<0.01$ versus LPS group.

Molecular modeling

To propose a binding mode for these new kynurenamine derivatives (**5a–o**) to i/nNOS, we performed docking and molecular dynamics (MD) simulation studies. The main descriptive pose obtained by docking for this family of compounds within iNOS (PDB ID: 3NW2)[26] is illustrated in Figure 4a with compound **5n**. According to this pose, interactions with the protein occur in three ways: 1) each urea nitrogen is hydrogen bonded to a carboxylate moiety of the heme group, 2) the 2″-NH_2 group of **5n** interacts with the Glu 371 side chain by means of two hydrogen bonds, and 3) the phenyl ring is situated below the heme group, establishing a π–cation interaction, and is surrounded by hydrophobic residues such as Phe 363, Val 346, and Pro 344.

On the other hand, Figure 4b shows the main pose adopted by most compounds within nNOS (PDB ID: 1QW6).[27] In this case, only one hydrogen bond is formed between the urea amine group of **5n** and the carboxylate group of Glu 592. The urea moiety is surrounded by a polar environment formed by three arginine residues (Arg 596, Arg 603 and Arg 481). It is noteworthy that the phenyl is now located below the heme group in a different position with respect to that observed in iNOS, allowing the chloride atom of the phenyl group to interact with Trp 587.

With regard to the differences found within the series of compounds **5a–o**, the major variations observed in their interaction with the binding site are in the π–cation interaction between the aromatic ring and the heme group, together with the hydrogen bonding network involving the urea moiety. In particular, those compounds bearing a phenyl group with an orientation that is too inclined with respect to the heme group lose activity. In addition, the establishment of two hydrogen bonds through the urea moiety reinforces the interaction and hence, the activity.

Next, we performed molecular dynamics (MD) simulations of iNOS and nNOS in complex with compound **5n** to take into account the flexibility of the protein (Figure 5). The analysis of the trajectory (Figure 5a) showed that those interactions described previously between the NH_2 group of **5n** and Glu 371 from one side, and between the heme carboxylate moiety with the **5n** urea moiety from the other side, were retained during the MD simulations. However, Figure 5b shows new hydrogen bonds between the urea residue and the heme carboxylate moiety. Furthermore, the main differences between the MD simulations of both isoforms with **5n** were essentially the new additional stabilizing interactions that **5n** establishes with residues Gln 257 and Arg 260 (iNOS), located at the entrance of the binding site, together with stacking with the heme group. In particular, the conformation of Gln 257 is controlled by the Arg 260 side chain orientation which, in turn, depends on the mutation of Thr 277 in iNOS and Asn 498 in nNOS.[28] These interactions, detected from the simulation process, could explain the iNOS selectivity shown by compounds like **5n** and the good nNOS inhibition observed for some compounds.

The binding of **5n** to iNOS was more favorable than to nNOS (-31.8 ± 0.8 versus -27.3 ± 2.2 kcal mol^{-1}, respectively), due to the great contribution of the π-stacking interaction with the heme group. Finally, the binding energy per residue (Table 3) observed for Gln 478 and Arg 481 (nNOS) with **5n** was less favorable than for the corresponding residues in iNOS (Gln 257 and Arg 260).

Conclusions

Herein we report the synthesis of fifteen novel urea and thiourea kynurenamine derivatives **5**, each with different substituents in the aromatic ring and the urea or thiourea moiety. In addition, we evaluate the nNOS and iNOS activity of these new structures. In general, the compounds had better inhibitory ac-

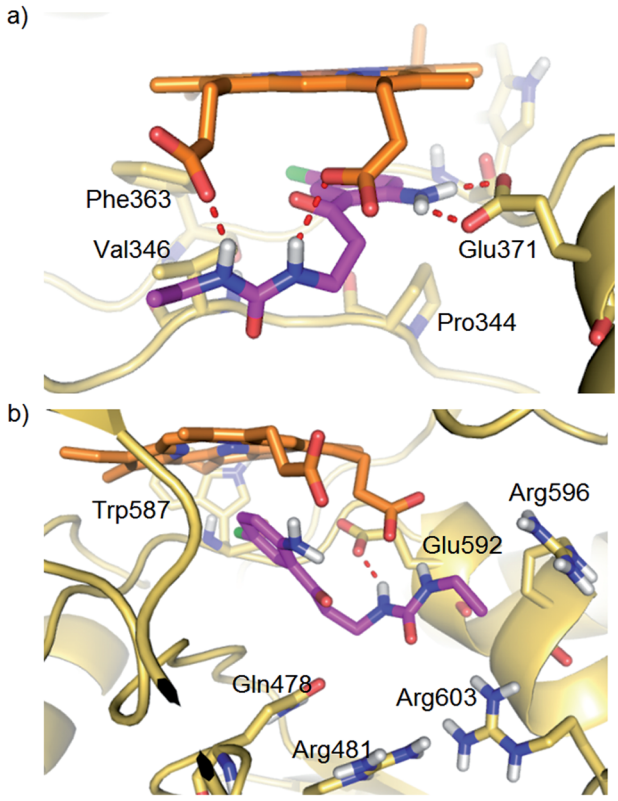

Figure 4. Detailed view of the main poses obtained for compound **5n** in the a) iNOS and b) nNOS binding sites. Dotted lines indicate hydrogen bond interactions between the ligand and residues of the enzyme.

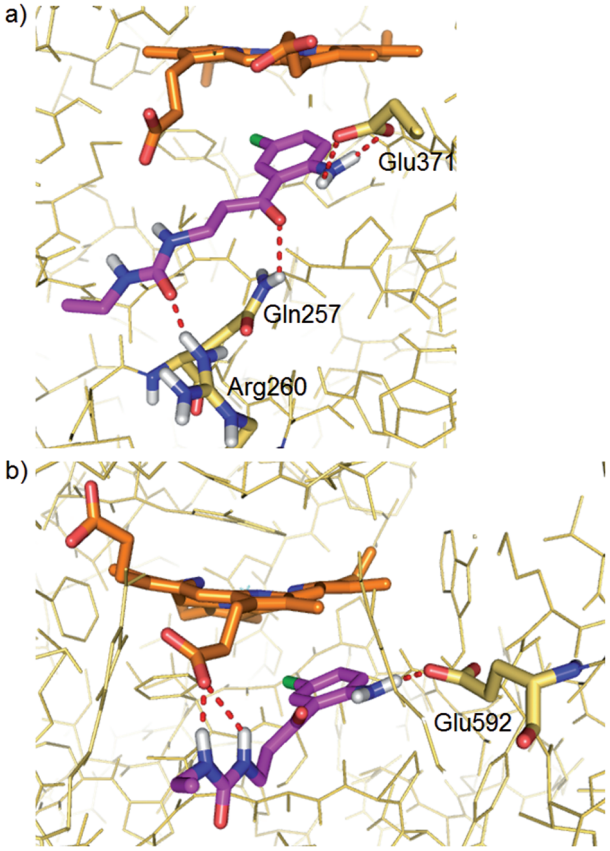

Figure 5. Image of a) **5n**–iNOS and b) **5n**–nNOS complexes taken from both average structures obtained from each MD simulation. Dotted lines indicate hydrogen bond interactions between the ligand and the residues of the enzyme.

Table 3. Calculated binding energy per residue of iNOS/nNOS with compound **5n**.[a]

iNOS		nNOS	
Residue	E [kcal mol^{-1}]	Residue	E [kcal mol^{-1}]
Heme	−11.8 ± 0.4	Heme	−6.2 ± 0.5
Pro 344	−2.5 ± 0.1	Pro 565	−2.6 ± 0.1
Glu 371	−2.5 ± 0.1	Glu 592	−6.5 ± 0.2
Gln 257	−2.5 ± 0.1	Gln 478	−0.6 ± 0.7
Val 346	−2.0 ± 0.1	Val 567	−1.3 ± 0.1
Arg 260	−1.3 ± 0.1	Arg 481	−0.4 ± 0.2
Trp 366	−0.9 ± 0.0	Trp 587	−1.2 ± 0.1
Gly 365	−0.7 ± 0.1	Gly 586	−0.7 ± 0.0
Phe 363	−0.7 ± 0.1	Phe 584	−0.9 ± 0.0

[a] Data are the mean ± SD of the calculated binding energies along the MD simulation (single run).

tivity against iNOS than nNOS, and derivatives with a withdrawing substituent in the aromatic ring were the best inhibitors. Thioureas similarly inhibited both isoenzymes, while ureas selectively inhibited iNOS. The urea **5n** was the most potent iNOS inhibitor and the most iNOS/nNOS-selective. This was confirmed by docking and MD simulations studies, which showed the more favorable orientation of **5n** in iNOS establishing good interactions with the enzyme. Also, this compound did not inhibit eNOS, demonstrating the selectivity necessary to avoid the adverse effects of hypertension. Consequently, this derivative could be an interesting starting point to find new therapeutic alternatives for inflammatory diseases.

Experimental Section

Chemistry

Melting points were determined using an Electrothermal-1 A-6301 apparatus and are uncorrected. Analytical thin layer chromatography was performed using Merck Kieselgel 60 F_{254} aluminum sheets, with the spots developed with UV light ($\lambda = 254$ nm). Flash chromatography was carried out using silica gel 60, 230–240 mesh (Merck), and the solvent mixture reported within parentheses was used as the eluent. ^{1}H NMR and ^{13}C NMR spectra were recorded on a Varian Inova Unity 300 spectrometer operating at 300.20 MHz for ^{1}H and 75.479 MHz for ^{13}C, on a Varian direct drive 400 spectrometer operating at 400.17 MHz for ^{1}H and 125.69 MHz for ^{13}C, and on a Varian direct drive 600 spectrometer operating at 600.24 MHz for ^{1}H and 150.95 MHz for ^{13}C in $CDCl_3$, CD_3OD, $(CD_3)_2CO$, and $(CD_3)_2SO$ at room temperature. The peaks are reported in ppm (δ) and are referenced to the residual solvent peak. High-resolution nano-assisted laser desorption/ionization (HR-NALDI) or electrospray ionization mass spectra (ESI-MS) were carried out on a Bruker Autoflex or a Waters LCT Premier mass spectrometer, respectively.

General method for the preparation of 1-(2-(2-(5-substituted-2-nitrophenyl)-1,3-dioxolan-2-yl)ethyl)-3-alkylthioureas and alkyl-

ureas, 9a–o: Hydrazine (95%, 6.18 mmol) was added to a solution of the corresponding phthalimide **7a–c** (2.06 mmol) in dry EtOH (60 mL). The mixture was held at reflux for 4.5 h, then cooled to room temperature and filtered, and the solvent was removed by evaporation. The crude residue was diluted with water (30 mL), basified with KOH, and extracted with EtOAc. The organic layer was dried over anhydrous Na_2SO_4, filtered, and concentrated to give amines **8a–c**. These intermediates were dissolved in anhydrous CH_2Cl_2 (9 mL) under argon atmosphere, and the corresponding alkylisocyanate or alkylisothiocyanate (4.12 mmol) was added dropwise. The reaction mixture was stirred overnight at room temperature. The crude mixture was concentrated and purified by flash chromatography (EtOAc/hexane, 1:2).

1-(2-(2-(2-Nitrophenyl)-1,3-dioxolan-2-yl)ethyl)-3-methylthiourea, 9a: Yellow solid (1.96 mmol, 95%); mp: 122–123 °C; ^{1}H NMR (600 MHz, $CDCl_3$): δ = 2.48 (t, 2H), 2.95 (s, 3H), 3.64–3.70 (m, 4H), 3.99–4.06 (m, 2H), 7.42–7.43 (m, 2H), 7.51 (ddd,1H), 7.59 ppm (d, 1H); ^{13}C NMR (150 MHz, $CDCl_3$): δ = 30.3, 38.1, 40.0, 65.0, 109.7, 123.5, 128.4, 129.8, 131.6, 134.7, 149.5, 180.8 ppm; HRMS *m/z* $[M+H]^+$ calcd for $C_{13}H_{18}N_3O_4S$: 312.1018, found: 312.1016.

1-(2-(2-(2-Nitrophenyl)-1,3-dioxolan-2-yl)ethyl)-3-ethylurea, 9d: White solid (1.46 mmol, 71%); mp: 168–169 °C; ^{1}H NMR (300 MHz, $CDCl_3$): δ = 1.12 (t, 3H), 2.36 (t, 2H), 3.17 (q, 2H), 3.36 (t, 2H), 3.62–3.67 (m, 2H), 3.96–4.02 (m, 2H), 7.37–7.42 (m, 2H), 7.45–7.52 (m, 1H), 7.55–7.60 ppm (m, 1H); ^{13}C NMR (75 MHz, $CDCl_3$): δ = 15.6, 35.7, 39.4, 65.1, 109.5, 123.4, 128.6, 129.7, 131.5, 135.2, 149.7, 158.5 ppm; HRMS *m/z* $[M+H]^+$ calcd for $C_{14}H_{20}N_3O_5$: 332.1228, found: 332.1222.

1-(2-(2-(5-Methoxy-2-nitrophenyl)-1,3-dioxolan-2-yl)ethyl)-3-methylthiourea, 9f: Yellow oil (1.48 mmol, 72%); ^{1}H NMR (300 MHz, $CDCl_3$): δ = 2.50–2.55 (m, 2H), 2.95 (d, 3H), 3.65–3.73 (m, 4H), 3.85 (s, 3H), 3.99–4.04 (m, 2H), 5.97 (bs), 6.43 (bs), 6.86 (dd, 1H), 7.06 (d, 1H), 7.48 ppm (d, 1H); ^{13}C NMR (75 MHz, $CDCl_3$): δ = 30.5, 38.0, 40.4, 56.2, 65.1, 109.5, 113.4, 114.3, 126.2, 137.7, 143.0, 161.9, 182.2 ppm; HRMS *m/z* $[M+Na]^+$ calcd for $C_{14}H_{19}N_3O_5SNa$: 364.0940, found: 364.0943.

1-(2-(2-(5-Methoxy-2-nitrophenyl)-1,3-dioxolan-2-yl)ethyl)-3-ethylurea, 9i: Yellow oil (1.38 mmol, 67%); ^{1}H NMR (300 MHz, $CDCl_3$): δ = 0.92 (t, 3H), 2.72 (t, 2H), 3.30 (q, 2H), 3.36 (t, 2H), 3.63–3.67 (m, 1H), 3.84 (s, 3H), 4.15–4.20 (m, 2H), 6.48 (bs, 2H), 6.84 (dd, 1H), 7.13 (d, 1H), 7.46 ppm (d, 1H); ^{13}C NMR (75 MHz, $CDCl_3$): δ = 15.5, 35.6, 39.0, 41.8, 55.6, 64.8, 109.5, 113.2, 114.1, 125.7, 137.6, 144.9, 158.6, 161.4 ppm; HRMS *m/z* $[M+H]^+$ calcd for $C_{15}H_{22}N_3O_6$: 340.1416, found: 340.1427.

1-(2-(2-(5-Chloro-2-nitrophenyl)-1,3-dioxolan-2-yl)ethyl)-3-methylthiourea, 9k: Yellow solid (1.40 mmol, 68%); mp: 164–165 °C; ^{1}H NMR (300 MHz, $CDCl_3$): δ = 2.45–2.49 (m, 2H), 2.95 (s, 3H), 3.67–3.73 (m, 4H), 4.02–4.06 (m, 2H), 7.39–7.40 (m, 2H), 7.57–7.59 ppm (m, 1H); ^{13}C NMR (75 MHz, $CDCl_3$): δ = 30.5, 38.1, 40.1, 65.3, 109.1, 125.2, 128.6, 130.0, 137.2, 137.9, 147.9, 181.7 ppm; HRMS *m/z* $[M+Na]^+$ calcd for $C_{13}H_{16}N_3O_4SClNa$: 346.0839, found: 346.0826.

1-(2-(2-(5-Chloro-2-nitrophenyl)-1,3-dioxolan-2-yl)ethyl)-3-ethylurea, 9n: Yellow oil (1.26 mmol, 61%); ^{1}H NMR (400 MHz, $CDCl_3$): δ = 1.10 (t, 3H), 2.35 (t, 2H), 3.17 (q, 2H), 3.29 (t, 2H), 3.65–3.67 (m, 2H), 4.02–4.04 (m, 2H), 7.36 −7.37 (m, 2H), 7.57–7.59 ppm (m, 1H); ^{13}C NMR (125 MHz, $CDCl_3$): δ = 15.3, 35.4, 35.4, 42.4, 64.9, 108.9, 124.7, 128.4, 129.4, 137.2, 137.3, 147.7, 158.8 ppm; HRMS *m/z* $[M+H]^+$ calcd for $C_{14}H_{19}N_3O_5Cl$: 344.7523, found: 344.7528.

General method for the preparation of 1-(3-(5-substituted-2-nitrophenyl)-3-oxopropyl)-3-alkylthioureas and alkylureas, 10a–o: A solution of concentrated HCl (13.5 mL, 12 N) was added to a solution of the corresponding dioxolane precursor **9a–o** (0.995 mmol) in CH_2Cl_2 (6.8 mL). The mixture was stirred for 4 h at room temperature and then quenched with an aqueous saturated solution of KOH until achieving a basic pH. The former aqueous phase was extracted with CH_2Cl_2 (3×15 mL), and the organic layers were washed with brine (1×15 mL), dried on anhydrous Na_2SO_4, filtered, and concentrated under vacuum. The crude mixture was purified by flash chromatography (EtOAc/hexane, 1:1).

1-(3-(2-Nitrophenyl)-3-oxopropyl)-3-methylthiourea, 10a: Yellow oil (0.61 mmol, 61%); ^{1}H NMR (400 MHz, $CDCl_3$): δ = 2.94 (s, 3H), 3.16–3.23 (m, 2H), 4.01–4.09 (m, 2H), 6.51 (bs, 2H), 7.42 (d, 1H), 7.57–7.61 (m, 1H), 7.69–7.71 (m, 1H), 8.06 ppm (d, 1H); ^{13}C NMR (125 MHz, $CDCl_3$): δ = 32.8, 39.5, 42.5, 124.5, 127.3, 131.1, 134.5, 137.2, 145.8, 181.5, 202.5 ppm; HRMS *m/z* $[M+H]^+$ calcd for $C_{11}H_{14}N_3O_3S$: 267.3049, found: 267.3052.

1-(3-(2-Nitrophenyl)-3-oxopropyl)-3-ethylurea, 10d: Yellow solid (0.61 mmol, 61%); mp: 133–134 °C; ^{1}H NMR (300 MHz, $CDCl_3$): δ = 1.10 (t, 3H), 3.03 (t, 2H), 3.17 (q, 2H), 3.62 (t, 2H), 7.40 (dd, 1H), 7.55–7.61 (m, 1H), 7.67–7.73 (m, 1H), 8.07 ppm (d, 1H); ^{13}C NMR (75 MHz, $CDCl_3$): δ = 15.6, 35.4, 35.6, 43.4, 124.7, 127.5, 131.0, 134.5, 137.6, 145.9, 158.5, 202.6 ppm; HRMS *m/z* $[M+Na]^+$ calcd for $C_{12}H_{15}N_3O_4Na$: 288.0954, found: 288.0960.

1-(3-(5-Methoxy-2-nitrophenyl)-3-oxopropyl)-3-methylthiourea, 10f: Yellow solid (0.83 mmol, 84%); mp: 176–180 °C; ^{1}H NMR (300 MHz, $(CD_3)_2CO$): δ = 2.92 (d, 3H), 3.15 (t, 2H), 3.87–3.93 (m, 2H), 3.96 (s, 3H), 6.91 (bs, 1H), 6.96 (bs, 1H), 7.06 (d, 1H), 7.16 (dd, 1H), 8.13 ppm (d, 1H); ^{13}C NMR (75 MHz, $(CD_3)_2CO$): δ = 30.2, 39.4, 42.4, 56.4, 112.5, 115.6, 127.2, 138.6, 140.8, 164.7, 184.3, 201.3 ppm; HRMS *m/z* $[M+Na]^+$ calcd for $C_{12}H_{15}N_3O_4SNa$: 320.0680, found: 320.0681.

1-(3-(5-Methoxy-2-nitrophenyl)-3-oxopropyl)-3-ethylurea, 10i: Yellow solid (0.73 mmol, 73%); mp: 146–147 °C; ^{1}H NMR (300 MHz, $CDCl_3$): δ = 1.14 (t, 3H), 2.99 (t, 2H), 3.21 (q, 2H), 3.65 (t, 2H), 3.90 (s, 3H), 6.75 (d, 1H), 6.98 (dd, 1H), 8.13 ppm (d, 1H); ^{13}C NMR (75 MHz, $CDCl_3$): δ = 15.4, 35.5, 35.9, 43.5, 56.6, 112.0, 115.4, 127.4, 138.2, 140.6, 158.7, 164.7, 202.6 ppm; HRMS *m/z* $[M+Na]^+$ calcd for $C_{13}H_{17}N_3O_5Na$: 318.1072, found: 318.1066.

1-(3-(5-Chloro-2-nitrophenyl)-3-oxopropyl)-3-methylthiourea, 10k: Yellow solid (0.61 mmol, 61%); mp: 129–130 °C; ^{1}H NMR (300 MHz, $CDCl_3$): δ = 2.96 (s, 3H), 3.17 (t, 2H), 4.07 (t, 2H), 7.36 (d, 1H), 7.56 (dd, 1H), 8.07 ppm (d, 1H); ^{13}C NMR (75 MHz, $CDCl_3$): δ = 29.9, 39.7, 42.6, 126.4, 127.5, 131.1, 138.9, 141.7, 144.0, 181.8, 201.1 ppm; HRMS *m/z* $[M+Na]^+$ calcd for $C_{11}H_{12}N_3O_3SClNa$: 324.0185, found: 324.0186.

1-(3-(5-Chloro-2-nitrophenyl)-3-oxopropyl)-3-ethylurea, 10n: White solid (0.62 mmol, 62%); mp: 149–150 °C; ^{1}H NMR (300 MHz, $CDCl_3$): δ = 1.14 (t, 3H), 3.04 (t, 2H), 3.20 (q, 2H), 3.64 (t, 2H), 4.87 (bs, 2H), 7.36 (d, 1H), 7.54 (dd, 1H), 8.06 ppm (d, 1H); ^{13}C NMR (75 MHz, $CDCl_3$): δ = 16.5, 36.7, 37.1, 44.5, 127.4, 128.8, 132.1, 142.8, 145.1, 160.0, 202.0; HRMS *m/z* $[M+H]^+$ calcd for $C_{12}H_{15}N_3O_4Cl$: 300.0760, found: 300.0751.

General method for the preparation of 1-(3-(2-aminophenyl-5-substituted)-3-oxopropyl)-3-alkylthioureas and alkylureas, 5a–o: A mixture of nitro precursor **10a–o** (0.93 mmol), iron powder (9.3 mmol), and $FeSO_4$ (0.93 mmol) in water (19.5 mL) was stirred and heated for 3 h at 95 °C. Next, the suspension was filtered through Celite and thoroughly washed with CH_2Cl_2. The aqueous phase was extracted with CH_2Cl_2 (3×15 mL). The merged organic layer was washed with brine (1×15 mL), dried (Na_2SO_4), filtered,

and evaporated under vacuum. The crude mixture was purified by flash chromatography (EtOAc/hexane, 1:1).

1-(3-(2-Aminophenyl)-3-oxopropyl)-3-methylthiourea, 5a: Yellow solid (0.76 mmol, 82%); mp: 127–128 °C; ^{1}H NMR (300 MHz, $CDCl_3$): $\delta = 2.96$ (s, 3H), 3.35 (t, 2H), 3.98–4.04 (m, 2H), 5.30 (bs, 2H), 6.30 (bs, 1H), 6.51 (bs, 1H), 6.64–6.72 (m, 2H), 7.28–7.34 (m, 1H), 7.73 ppm (dd, 1H); ^{13}C NMR (75 MHz, $CDCl_3$): $\delta = 30.3$, 38.5, 40.1, 116.3, 117.5, 117.6, 131.2, 135.0, 150.3, 182.2, 201.9 ppm; HRMS *m/z* $[M+Na]^+$ calcd mass for $C_{11}H_{15}N_3OSNa$: 260.0834, found: 260.0838; Anal. calcd for $C_{11}H_{15}N_3OS$: C 55.67, H 6.37, N 17.71, found: C 55.35, H 6.31, N 17.58.

1-(3-(2-Aminophenyl)-3-oxopropyl)-3-ethylurea, 5d: White solid (0.74 mmol, 80%); mp: 139–141 °C; ^{1}H NMR (300 MHz, $CDCl_3$): $\delta =$ 1.09 (t, 3H), 3.11–3.19 (m, 4H), 3.57 (t, 2H), 4.77 (bs, 4H), 6.59–6.66 (m, 2H), 7.24 (ddd, 1H), 7.69 ppm (dd, 1H); ^{13}C NMR (75 MHz, $CDCl_3$): $\delta = 15.4$, 35.4, 35.5, 39.4, 116.1, 117.4, 117.9, 131.2, 134.6, 150.2, 158.8, 202.0 ppm; HRMS *m/z* $[M+Na]^+$ calcd mass for $C_{12}H_{17}N_3O_2Na$: 258.1218, found: 258.1227. Anal. calcd for $C_{12}H_{17}N_3O_2$: C 61.26, H 7.28, N 17.86, found: C 61.53, H 7.55; N 17.46.

1-(3-(2-Amino-5-methoxyphenyl)-3-oxopropyl)-3-methylthiourea, 5f: Yellow solid (0.87 mmol, 94%); mp: 125–126 °C; ^{1}H NMR (300 MHz, $CDCl_3$): $\delta = 2.90$ (d, 3H), 3.27 (t, 2H), 3.74 (s, 3H), 3.93–4.01(m, 2H), 5.95 (bs, 2H), 6.27 (bs, 1H), 6.47 (bs, 1H), 6.60 (d, 1H), 6.95 (dd, 1H), 7.12 ppm (d, 1H); ^{13}C NMR (75 MHz, $CDCl_3$): $\delta = 30.4$, 38.9, 40.3, 56.3, 113.2, 117.5, 119.1, 124.6, 145.4, 150.5, 182.4, 201.6 ppm; HRMS *m/z*: $[M+Na]^+$ calcd mass for $C_{12}H_{17}N_3O_2SNa$: 290.0939, found: 290.0940. Anal. calcd for $C_{12}H_{17}N_3O_2S$: C 53.91, H 6.41, N 15.72, S 11.99, found: C 53.55; H 6.79, N 15.11, S 11.73.

1-(3-(2-Amino-5-methoxyphenyl)-3-oxopropyl)-3-ethylurea, 5i: Yellow solid (0.83 mmol, 89%); mp: 115–117 °C; ^{1}H NMR (300 MHz, $CDCl_3$): $\delta = 1.06$ (t, 3H), 3.10–3.18 (m, 4H), 3.57 (t, 2H), 3.74 (s, 3H), 5.21 (bs, 4H), 6.73 (d, 1H), 6.95 (dd, 1H), 7.16 ppm (d, 1H); ^{13}C NMR (75 MHz, $CDCl_3$): $\delta = 15.6$, 35.6, 35.6, 39.9, 56.2, 113.8, 119.3, 120.1, 123.5, 142.8, 151.5, 158.6, 201.9 ppm; HRMS *m/z* $[M+Na]^+$ calcd mass for $C_{13}H_{19}N_3O_3Na$: 288.1324, found: 288.1329. Anal. calcd for $C_{13}H_{19}N_3O_3$: C 58.85, H 7.22, N 15.84, found: C 59.17, H 7.55, N 15.57.

1-(3-(2-Amino-5-chlorophenyl)-3-oxopropyl)-3-methylthiourea, 5k: Yellow solid (0.65 mmol, 70%); mp: 166–168 °C; ^{1}H NMR (300 MHz, $(CD_3)_2SO$): $\delta = 2.76$ (s, 3H), 3.16 (t, 2H), 3.61–3.63 (m, 2H), 6.76 (d, 1H), 7.24 (dd, 1H), 7.40 (bs, 2H), 7.75 ppm (d, 1H); ^{13}C NMR (75 MHz, $(CD_3)_2SO$): $\delta = 31.1$, 38.8, 40.0, 117.8, 119.7, 121.7, 130.8, 134.7, 150.5, 181.4, 200.6 ppm; HRMS *m/z* $[M+H]^+$ calcd mass for $C_{11}H_{15}N_3OSCl$: 272.0624, found: 272.0609. Anal. calcd for $C_{11}H_{14}N_3OS$: C 48.61, H 5.19, N 15.46, found: C 53.63, H 6.20, N 12.57.

1-(3-(2-Amino-5-chlorophenyl)-3-oxopropyl)-3-ethylurea, 5n: Yellow solid (0.70 mmol, 75%); mp: 157–160 °C; ^{1}H NMR (300 MHz, $CDCl_3$): $\delta = 1.10$ (t, 3H), 3.13–3.21 (m, 4H), 3.58 (t, 2H), 4.59 (bs, 4H), 6.60 (d, 1H), 7.19 (dd, 1H), 7.63 ppm (d, 1H); ^{13}C NMR (75 MHz, $CDCl_3$): $\delta = 15.5$, 35.8, 35.8, 39.6, 118.6, 119.2, 120.8, 130.5, 135.0, 148.8, 158.6, 201.2 ppm; HRMS *m/z* $[M+Na]^+$ calcd mass for $C_{12}H_{16}N_3O_2ClNa$: 292.0829, found: 292.0835. Anal. calcd for $C_{12}H_{16}N_3O_2Cl$: C 53.43, H 5.98, N 15.58 found: C 53.11, H 5.64, N 15.36.

Biological assays

In vitro nNOS and iNOS activity determination: L-Arginine, L-citrulline, *N*-(2-hydroxymethyl)piperazine-*N*′-(2-ethanesulfonic acid) (HEPES), D,L-dithiothreitol (DTT), hypoxanthine-9-β-D-ribofuranoside (inosine), (ethylene glycol)-bis-(2-aminoethylether)-*N*,*N*,*N*′,*N*′-tetraacetic acid (EGTA), bovine serum albumin (BSA), Dowex-50W (50×8–200), FAD, NADPH, and 5,6,7,8-tetrahydro-L-biopterin dihydrochloride (H_4-biopterin), tris-(hydroxymethyl)aminomethane (Tris·HCl), and calcium chloride were obtained from Sigma–Aldrich Química (Spain). L-[^{3}H]arginine (47.4 Ci mmol^{-1}) was obtained from PerkinElmer (Spain). Calmodulin from bovine brain and recombinant iNOS and nNOS were obtained from Enzo Life Sciences (Spain).

i/nNOS activity was measured by the Bredt and Snyder method,[29] monitoring the conversion of L-[^{3}H]arginine to L-[^{3}H]citrulline. The final incubation volume was 100 μL and consisted of 10 μL of an aliquot of recombinant i/nNOS added to a buffer with a final concentration of 25 mM Tris·HCl, 1 mM DTT, 4 μM H_4-biopterin, 10 μM FAD, 0.5 mM inosine, 0.5 mg mL^{-1} BSA, 0.1 mM $CaCl_2$, 10 μM L-arginine, 10 μg mL^{-1} calmodulin (only for nNOS), and 50 nM L-[^{3}H]arginine, at pH 7.6 and 7.0 for iNOS and nNOS, respectively. The reaction was started by the addition of 10 μL of 7.5 mM NADPH and 10 μL of each kynurenamine derivative in EtOH (20%) to give a final concentration of 1 mM. The tubes were vortexed and incubated at 37 °C for 30 min. Control incubations were performed by the omission of NADPH. The reaction was halted by the addition of 400 μL of cold 0.1 M HEPES, 10 mM EGTA, and 0.175 mg mL^{-1} L-citrulline, pH 5.5. The reaction mixture was decanted into a 2 mL column packet with Dowex-50W ion-exchange resin (Na^+ form) and eluted with 1.2 mL water. L-[^{3}H]Citrulline was quantified by liquid scintillation spectroscopy. The retention of L-[^{3}H]arginine in this process was greater than 98%. Specific enzyme activity was determined by subtracting the control value, which usually amounted to less than 1% of the radioactivity added. The nNOS activity was expressed as pmol L-[^{3}H]citrulline produced per mg protein per min.

Tissue preparation and measurement of tension: This investigation conformed to the Guide for the Care and Use of Laboratory Animals published by the U.S. National Institutes of Health (NIH Publication No. 85–23, revised 1996) and with the principles outlined in the Declaration of Helsinki and approved by our institutional review board. Male Wistar rats (250–300 g), obtained from Harlam Laboratories SA (Barcelona, Spain), were euthanized by a quick blow on the head followed by exsanguination. The descending thoracic aortic rings were dissected, and the endothelium was removed mechanically and incubated in Krebs solution (118 mM NaCl, 4.75 mM KCl, 25 mM $NaHCO_3$, 1.2 mM $MgSO_4$, 2 mM $CaCl_2$, 1.2 mM KH_2PO_4, and 11 mM glucose) at 37 °C and gassed with 95% O_2 and 5% CO_2 for 20 h in a cell culture incubator in the absence or presence of *Escherichia coli* 055:B5 lipopolysaccharide (LPS, 1 μg mL^{-1}) (Sigma–Aldrich, Spain). Rings were then mounted in organ chambers filled with Krebs solution and were stretched to 2 g of resting tension by means of two L-shaped stainless steel wires inserted into the lumen and attached to the chamber and to an isometric force-displacement transducer (UF-1, Cibertec, Spain) and recorded in a recording and analysis system (MacLab AD Instruments), as described previously.[30] After equilibration of aortic rings, concentration–response curves for noradrenaline (NA, 10^{-9}–10^{-5} M) were performed by increasing the concentration in the organ chamber in cumulative increments after a steady-state response was reached with each increment. In some experiments, the non-selective NOS inhibitor, NG-nitro-arginine methyl ester (L-

NAME, 3×10^{-4} M), compound **5n** (10^{-4} M), or vehicle (DMSO) alone were added to the organ chamber 30 min before the addition of NA. The rings were then removed from the organ chambers, air-dried for 24 h, and weighed. The contraction was expressed in grams of force per milligram of dried tissue. The area under the concentration–response curve (AUC) was measured.

In another experiment, aortic rings with a functional endothelium were incubated with vehicle or **5n** (1 mM) for 30 min and contracted with NA (1 μM). Once a plateau contraction was reached, a concentration–response curve was constructed by cumulative addition of acetylcholine. Results are expressed as percentage of NA-evoked contraction. *n* reflects the number of aortic rings from different rats.

Quantification of NO in human umbilical vein endothelial cells (HUVECs): Endothelial cells were isolated from human umbilical cord veins using a previously reported method with several modifications.[31] The cells were cultured in Medium 199 with 20% fetal bovine serum and penicillin/streptomycin (2 mM), amphotericin B (2 mM), glutamine (2 mM), HEPES (10 mM), endothelial cell growth supplement (30 μg mL^{-1}), and heparin (100 mg mL^{-1}) under 5% CO_2 at 37 °C. HUVECs were then used to measure NO production by diaminofluorescein-2 (DAF-2) fluorescence, as described previously.[31] Briefly, cells were incubated for 30 min in the presence of **5n** at a concentration of 1 mM. After this period, cells were washed with PBS and then were pre-incubated with L-arginine (100 μM in PBS for 5 min at 37 °C). Subsequently, DAF-2 (0.1 μM) was incubated for 2 min, then the calcium ionophore calimycin (A23187, 1 μM) was added for 30 min, and cells were incubated in the dark at 37 °C. Fluorescence (arbitrary units) was then measured using a spectrofluorimeter (Fluorostart, BMG Labtechnologies, Offenburg, Germany). The auto-fluorescence was subtracted from each value. The area under the time–fluorescence curve (AUC) was measured.

Statistical analysis: Data are expressed as the mean ± SEM. Statistically significant differences between groups were calculated by Students' t test for unpaired observations or for multiple comparisons. ANOVA, followed by the Newmane–Keuls multiple range test, was used. A $p < 0.05$ was considered statistically significant.

Docking and molecular dynamics (MD) simulations

The Maestro suite of programs (Schrödinger, LCC[32]) was used for the docking studies. The Cartesian coordinates for the two proteins, iNOS and nNOS, were obtained from the Protein Data Bank and treated with the Protein Preparation Wizard module[33] of Maestro. The 3D structures of the conformers of compounds **5a–o** were generated using the program LigPrep[34] after taking their structures from fragment libraries and optimizing using the Macromodel module. Rigid docking was performed using Glide with a Standard Precision (SP) protocol. Figure were built using PyMOL.[35]

Unrestrained MD simulations were carried out with the AMBER 12 software suite[36] in explicit solvent using the AMBER force field leaprc.ff10. The PDB2PQR tool[37,38] was used to estimate the most probable protonation states of titratable residues in the proteins at pH 7.0 and also to add all missing hydrogen atoms. Parameters for the prosthetic heme group were obtained from Giammona.[39] Parameters for compound **5n** as well as for H_4B were calculated using the antechamber module and the generalized AMBER force field with AM1-BCC charges.

Each enzyme–inhibitor complex was immersed in a cubic box of TIP3P water molecules with a minimum distance of 12 Å from any atom to the edge. The system was neutralized by incorporating the necessary amount of sodium ions. Particle Mesh Ewald method for long-range electrostatic interactions, together with standard periodic boundary conditions, were used. The SHAKE algorithm was applied to reach an integration step of 2.0 fs.

Before the simulation, the system was energetically minimized with a protocol of: 2000 steps of steepest descent, followed by 3000 steps of conjugate gradient. In this protocol, hydrogen atoms were first optimized, freezing the rest of the system, then only the water molecules were allowed to move, and finally the whole system was allowed to move. Next, the system was heated to 300 K in 20 ps at 1 atm using the Berendsen thermostat and a restraint constant on the alpha carbon of protein residues, ligands, and cofactors. The restraint was then decreased slowly in the equilibration step. Finally, 2 ns of production simulation were performed, collecting the coordinates of the system at each 1 ps. The binding free energy was calculated using the MM-ISMSA model,[40] and the estimated error was obtained with the block averaging method implemented in the *g analyse* tool of the GROMACS suite.[41]

Acknowledgements

This work was supported in part by the Instituto de Salud Carlos III through grant FI11/00432 and project RIC RD12/0042/0011.

Keywords: biological activity · inhibitors · kynurenamines · molecular modeling · nitric oxide synthase

[1] S. Moncada, R. M. Palmer, E. A. Higgs, *Pharmacol. Rev.* **1991**, *43*, 109–142.
[2] O. W. Griffith, D. J. Stuehr, *Annu. Rev. Physiol.* **1995**, *57*, 707–734.
[3] L. J. Roman, P. Martásek, B. S. Masters, *Chem. Rev.* **2002**, *102*, 1179–1189.
[4] R. G. Knowles, S. Moncada, *Biochem. J.* **1994**, *298*, 249–258.
[5] W. K. Alderton, C. E. Cooper, R. G. Knowles, *Biochem. J.* **2001**, *357*, 593–615.
[6] J. T. Groves, C. C. Wang, *Curr. Opin. Chem. Biol.* **2000**, *4*, 687–695.
[7] F. Aktan, *Life Sci.* **2004**, *75*, 639–653.
[8] M. A. Smith, M. Vasak, M. Knipp, R. J. Castellani, G. Perry, *Free Radical Biol. Med.* **1998**, *25*, 898–902.
[9] G. T. Liberatore, V. Jackson-Lewis, S. Vukosavic, A. S. Mandir, M. Vila, W. G. McAuliffe, V. L. Dawson, T. M. Dawson, S. Przedborski, *Nat. Med.* **1999**, *5*, 1403–1409.
[10] P. J. Norris, H. J. Waldvogel, R. L. Faull, D. R. Love, P. C. Emson, *Neuroscience* **1996**, *72*, 1037–1047.
[11] N. K. Wong, M. J. Strong, *Eur. J. Cell Biol.* **1998**, *77*, 338–343.
[12] C. O. Bingham III, *J. Rheumatol. Suppl.* **2002**, *65*, 3–9.
[13] K. D. Kröncke, K. Fehsel, V. Kolb-Bachofen, *Clin. Exp. Immunol.* **1998**, *113*, 147–156.
[14] S. Taddei, A. Virdis, L. Ghiadoni, I. Sudano, A. Salvetti, *J. Cardiovasc. Pharmacol.* **2001**, *38*, S11–S14.
[15] C. Napoli, F. de Nigris, S. Williams-Ignarro, O. Pignalosa, V. Sica, L. J. Ignarro, *Nitric Oxide* **2006**, *15*, 265–279.
[16] J. León, F. Vives, E. Crespo, E. Camacho, A. Espinosa, M. A. Gallo, G. Escames, D. Acuña-Castroviejo, *J. Neuroendocrinol.* **1998**, *10*, 297–302.
[17] J. León, M. Macías, G. Escames, E. Camacho, H. Khaldy, M. Martín, A. Espinosa, M. A. Gallo, D. Acuña-Castroviejo, *Mol. Pharmacol.* **2000**, *58*, 967–975.
[18] E. Camacho, J. Leon, A. Carrion, A. Entrena, G. Escames, H. Khaldy, D. Acuña-Castroviejo, M. A. Gallo, A. Espinosa, *J. Med. Chem.* **2002**, *45*, 263–274.

[19] A. Entrena, M. E. Camacho, M. D. Carrión, L. C. López-Cara, G. Velasco, J. León, G. Escames, D. Acuña-Castroviejo, V. Tapias, M. A. Gallo, A. Vivó, A. Espinosa, *J. Med. Chem.* **2005**, *48*, 8174 – 8181.
[20] M. E. Camacho, J. León, A. Entrena, G. Velasco, M. D. Carrión, G. Escames, A. Vivó, D. Acuña-Castroviejo, M. A. Gallo, A. Espinosa, *J. Med. Chem.* **2004**, *47*, 5641 – 5650.
[21] V. Tapias, G. Escames, L. C. López, A. López, E. Camacho, M. D. Carrión, A. Entrena, M. A. Gallo, A. Espinosa, D. Acuña-Castroviejo, *J. Neurosci. Res.* **2009**, *87*, 3002 – 3010.
[22] M. D. Carrión, M. Chayah, A. Entrena, A. López, M. A. Gallo, D. Acuña-Castroviejo, M. E. Camacho, *Bioorg. Med. Chem.* **2013**, *21*, 4132 – 4142.
[23] J. S. Fortin, J. Lacroix, M. Desjardins, A. Patenaude, E. Petitclerc, R. C. Gaudreault, *Bioorg. Med. Chem.* **2007**, *15*, 4456 – 4469.
[24] C. Szabó, J. A. Mitchell, C. Thiemermann, R. J. Vane, *Br. J. Pharmacol.* **1993**, *108*, 786 – 792.
[25] A. L. Weigert, E. M. Higa, M. Niederberger, I. F. McMurtry, M. Raynolds, R. W. Schrier, *J. Am. Soc. Nephrol.* **1995**, *5*, 2067 – 2072.
[26] U. Grädler, T. Fuchss, W.-R. Ulrich, R. Boer, A. Strub, C. Hesslinger, C. Anézo, K. Diederichs, A. Zaliani, *Bioorg. Med. Chem. Lett.* **2011**, *21*, 4228 – 4232.
[27] R. Fedorov, E. Hartmann, D. K. Ghosh, I. Schlichting, *J. Biol. Chem.* **2003**, *278*, 45818 – 45825.
[28] L. C. López-Cara, M. D. Carrión, A. Entrena, M. A. Gallo, A. Espinosa, A. López, G. Escames, D. Acuña-Castroviejo, M. E. Camacho, *Eur. J. Med. Chem.* **2012**, *50*, 129 – 139.
[29] D. S. Bredt, S. H. Snyder, *Proc. Natl. Acad. Sci. USA* **1990**, *87*, 682 – 685.
[30] J. Duarte, M. A. Ocete, F. Pérez-Vizcaino, A. Zarzuelo, J. Tamargo, *Eur. J. Pharmacol.* **1997**, *338*, 25 – 33.
[31] R. Jiménez, M. Sánchez, M. J. Zarzuelo, M. Romero, A. M. Quintela, R. López-Sepúlveda, P. Galindo, M. Gómez-Guzmán, J. M. Haro, A. Zarzuelo, F. Pérez-Vizcaino, J. Duarte, *J. Pharmacol. Exp. Ther.* **2010**, *332*, 554 – 561.
[32] Schrödinger Suite **2012**: Update 2.
[33] Schrödinger Suite **2012**: Protein Preparation Wizard, Epik version 2.3; Impact version 5.8; Prime version 3.1, Schrödinger LLC, New York, NY (USA).
[34] Lig Prep version 2.5, Schrödinger LLC, New York, NY (USA), **2012**.
[35] PyMOL Molecular Graphics System, version 1.4, Schrödinger LLC, New York, NY (USA).
[36] AMBER 12: D. A. Case, T. A. Darden, T. E. Cheatham III, C. L. Simmerling, J. Wang, R. E. Duke, R. Luo, R. C. Walker, W. Zhang, K. M. Merz, B. Roberts, S. Hayik, A. Roitberg, G. Seabra, J. Swails, A. W. Goetz, I. Kolossvai, K. F. Wong, F. Paesani, J. Vanicek, R. M. Wolf, J. Liu, X. Wu, S. R. Brozell, T. Steinbrecher, H. Gohlke, Q. Cai, X. Ye, J. Wang, M. J. Hsieh, G. Cui, D. R. Roe, D. H. Mathews, M. G. Seetin, R. Salomon-Ferrer, C. Sagui, V. Babin, T. Luchko, S. Gusarov, A. Kovalenko, P. A. Kollman, University of California, San Francisco, **2012**.
[37] T. J. Dolinsky, P. Czodrowski, H. Li, J. E. Nielsen, J. H. Jensen, G. Klebe, N. A. Baker, *Nucleic Acids Res.* **2007**, *35*, W522 – W525.
[38] T. J. Dolinsky, J. E. Nielsen, J. A. McCammon, N. A. Baker, *Nucleic Acids Res.* **2004**, *32*, W665 – W667.
[39] Parameters around the iron atom are appropriate for a six-coordinate (ligand bound) hemoglobin/myoglobin. Force field parameters were adapted from D. A. Giammona, PhD thesis, University of California, Davis, **1984**.
[40] J. Klett, A. Núñez-Salgado, H. G. Dos Santos, A. Cortés-Cabrera, A. Perona, R. Gil-Redondo, D. Abia, F. Gago, A. Morreale, *J. Chem. Theory Comput.* **2012**, *8*, 3395 – 3408.
[41] S. Pronk, S. Páll, R. Schulz, P. Larsson, P. Bjelkmar, R. Apostolov, M. R. Shirts, J. C. Smith, P. M. Kasson, D. Van der Spoel, B. Hess, *Bioinformatics* **2013**, *29*, 845 – 854.

Received: January 9, 2015
Published online on March 20, 2015